JAPANESE JOURNAL OF APPLIED PHYSICS
VOL. 29, NO. 6, JUNE, 1990, pp. 1139–1142

Effect of Impurity Segregation on Crystal Morphology of Y-Bar Synthetic Quartz

Fumiko IWASAKI, Armando H. SHINOHARA, Hideo IWASAKI and Carlos K. SUZUKI

Laboratório de Quartzo, Departamento de Materiais, Faculdade de Engenharia de Campinas, UNICAMP, 13100 Campinas, São Paulo, Brasil

(Received January 30, 1990; accepted for publication April 21, 1990)

The effects of Al and H impurities on the crystal morphology of *Y*-bar synthetic quartz were studied. The growth velocities perpendicular to the *Y*-axis were evaluated in relation to the Al and H impurity segregations on the growth interfaces. It was found that the $-X$-growth region has the highest H content and shows the lowest growth velocity, due to the effect of H_2O adsorbed on the growth interface in hydrothermal solution. Therefore, the $-X$-face, $(\bar{1}\bar{1}20)$, always becomes larger in size. Al has a selective effect on the $(11\bar{2}2)$ and $(\bar{1}\bar{1}2\bar{2})$ faces to suppress the growth velocities and thus is important for crystal morphology. The growth velocities perpendicular to these faces, however, are controllable by the Al impurity content in the nutrient.

KEYWORDS: synthetic quartz, Al impurity, H impurity, morphology, hydrothermal growth, atomic absorption spectroscopy, infrared spectroscopy, X-ray topography

§1. Introduction

Synthetic quartz grown on a seed of a *Y*-bar or a *Z*-plate with a long *Y*-direction shows sector-shape growth regions on the *Y*-cut section. It is known that each growth region has a different impurity content depending on the growth directions. For example, the Al impurity content was found to increase in the order *Z*-region $<+X$-region $<-X$-region $<S$-region.[1] On the other hand, the sequence *Z*-region $<+X$-region $<S$-region $<-X$-region was observed in the case of the H impurity content.[2,3] Segregation of Al and H impurities is supposed to be related to growth anisotropy and thus to modify crystal morphology. It was reported that the volume ratio of the *S*-region to the whole crystal increased with increasing Al content in the nutrient.[1,4,5] However, the effects of impurities on crystal morphology have not yet been understood in detail.

In the present study, first, the morphology of several *Y*-bar synthetic quartzes was observed by X-ray topography. Next, impurity segregation and its effect on crystal growth velocity were observed using synthetic quartz grown on seeds with various orientations. The effects of the Al and H impurities on crystal morphology were discussed.

§2. Experimental

The crystals used in the present study, except Al-doped synthetic quartz, were grown under the standardized conditions of commercial synthetic quartz at ABC XTAL in Brazil. The growth conditions are the same as those reported in the previous paper.[1] Al-doped synthetic quartz prepared at Kinseki Ltd. in Japan was grown in Na_2CO_3 solution containing Al_2O_3. The ratio of Al to nutrient SiO_2 was evaluated to be about 1000 ppm, if Al content in the nutrient was neglected.

The X-ray topography adopted for morphological observations was the double-crystal method with non-parallel setting using Cu $K\alpha_1$ radiation.[4,5]

Table I. List of Seeds.

Seeds	Growth interfaces
X-cut	$+X$ $(11\bar{2}0)$
	$-X$ $(\bar{1}\bar{1}20)$
Z-cut	$+Z$ (0001)
	$-Z$ $(000\bar{1})$
S-cut	$+S$ $(11\bar{2}1)$
	$-S$ $(\bar{1}\bar{1}2\bar{1})$
ξ-cut*	$+\xi$ $(11\bar{2}2)$
	$-\xi$ $(\bar{1}\bar{1}2\bar{2})$

*$(11\bar{2}2)$ is defined as ξ by Frondel.[6]
Here, the plate parallel to $(11\bar{2}2)$ is called "ξ-cut".

Impurity segregation in relation to the growth directions was evaluated using samples grown on seeds with various orientations, as shown in Table I. Analyses of Al and H impurities were carried out for the sector-shape regions grown perpendicular to the seed plate in each crystal. Al impurity analysis was performed by atomic absorption spectroscopy using Model AA-670, Shimadzu Corporation. For H impurity analysis, infrared absorption spectroscopy was adopted at room temperature using IR-M80, Carl Zeiss-Jena. Optically polished *Y*-cut plates with 10 mm thickness were used for infrared spectroscopy. The calibration method for quantitative analysis will be explained in the following section.

§3. Results and Discussion

3.1 *Morphological observation by X-ray topography*

Figure 1 shows X-ray topographs of *Y*-cut plates. Figures 1(a) and 1(b) correspond to synthetic quartzes grown on conventional *Y*-bar seeds using the nutrient with Al contents of 30 ppm and 240 ppm, respectively. In both cases, *S*-regions occur at the corners of the seed and develop between the *Z*- and the $+X$-regions. It is clear that Al has the effect of increasing the volume ratio of the

S-region to the whole crystal. Therefore, the Al impurity has a selective effect of changing the growth velocity depending on the crystal faces. The S-region of synthetic quartz grown by the nutrient with lower Al content consists of two subregions, S_1 and S_2, as shown in Fig. 1(a). By contrast, only the S_1-region is observed in Fig. 1(b). Therefore, it is interpreted that Al has the effect of increasing the volume of the S_1-region. The growth interfaces of the S_1- and S_2-regions are faceted surfaces. The faceted surface of the S_1-region makes an angle of about 42° with the Z-axis, and thus corresponds to $(11\bar{2}2)$. The angle between the growth interface of the S_2-region and Z-axis does not have a deffinite value, but distributes between 27° and 30°. The S-face which is frequently observed in natural quartz corresponds to $(11\bar{2}1)$ and makes an angle of 24° with the Z-axis. The S-region in synthetic quartz is unrelated to $(11\bar{2}1)$, although for a long time, it had been called the S-region. This fact was also reported in the study of Al-doped synthetic quartz.[7] Figure 2 shows the X-ray topograph of synthetic quartz grown on the cylindrical Y-bar seed using the nutrient with Al content of 30 ppm. The two additional regions are observed between the Z- and $-X$-regions. These exist at the opposite directions of the S-regions. Therefore, we will call the S-region and the new region the $+S$- and $-S$-regions, respectively. It is observed that even though the surface of the cylindrical Y-bar contains faces all parallel to the Y-axis, only Z-, $+X$-, $-X$-, $+S$- and $-S$-regions are grown from the seed surface. This fact indicates that the growth directions of these regions have slower growth velocities within the perpendicular direction of the Y-axis. Figure 3(a) shows a part of the X-ray topograph of the Y-cut plate taken from Al-doped syn-

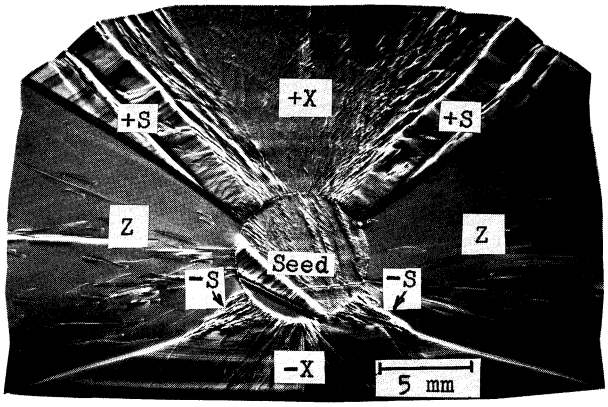

Fig. 2. X-ray topograph of Y-cut plate taken from synthetic quartz grown on the cylindrical Y-bar seed (reversed print). This seed contains $+X$, S and Z-regions on the original crystal. Topograph was taken in the Laue case with $(20\bar{2}0)$ reflections.

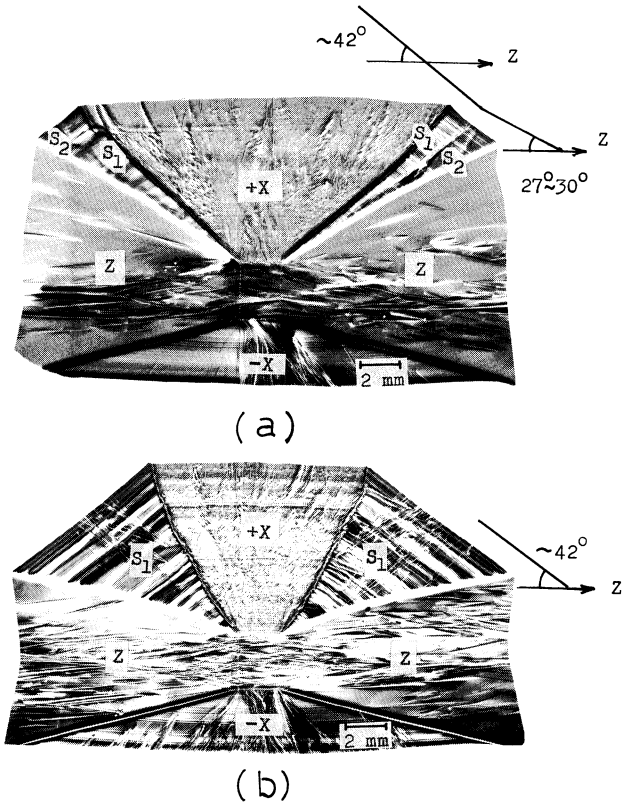

Fig. 1. X-ray topographs of Y-cut plates (reversed print). Topographs were taken in the Laue case with $(20\bar{2}0)$ reflections. The angle between the growth interface and Z-axis can be obtained from this topograph because the reduction rate of the Z-axis is about 0.9. (a) Synthetic quartz grown by the nutrient with Al of 30 ppm. (b) Synthetic quartz grown by the nutrient with Al of 240 ppm.

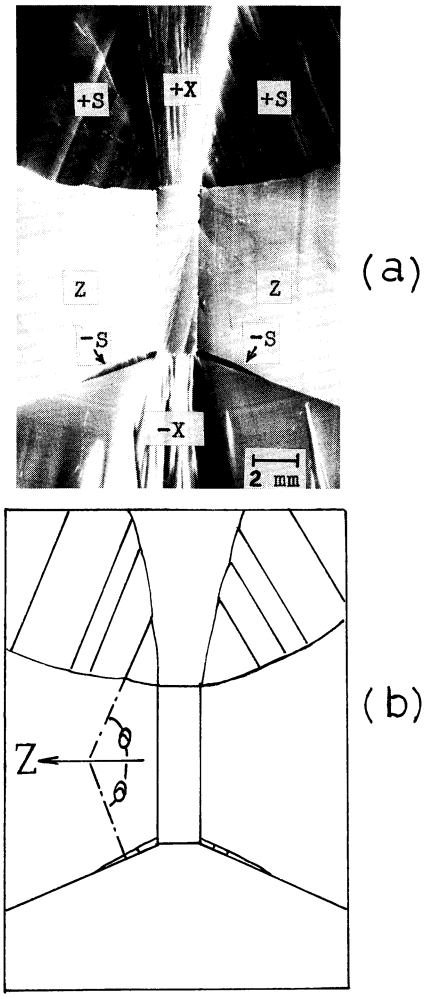

Fig. 3. Al-doped synthetic quartz. (a) X-ray topograph of Y-cut plate (reversed print). Topograph was taken in the Bragg case with $(1\bar{1}00)$ reflections. (b) Schematic figure.

thetic quartz. The topograph was taken in the Bragg case. Small $-S$-regions exist between the Z- and $-X$-regions. The growth layers due to the fluctuation of the impurity content are observed in both $+S$- and $-S$-regions. The angle between the growth layers and Z-axis is approximately the same in each case, even though the inclination orientations are opposite, as shown schematically in Fig. 3(b).

From the above results, it is interpreted that Al has the selective effect of suppressing the growth velocity on both the $(11\bar{2}2)$ and $(\bar{1}\bar{1}22)$ faces. Therefore, the $(11\bar{2}2)$ and $(\bar{1}\bar{1}22)$ faces become morphologically important when the adsorption of Al on the growth interfaces participates in the growth process. However, Al has a stronger effect on $(11\bar{2}2)$ than on $(\bar{1}\bar{1}22)$, because $-S$-regions occur at the conners of the conventional Y-bar seed only in the case of Al-doped synthetic quartz.

3.2 *Impurity segregation and growth velocities*

In order to evaluate impurity segregation and its effect on growth velocity, synthetic quartzes grown on the X-cut, the ξ-cut, the S-cut and the Z-cut seeds were used. ξ-cut seed grows on the $(11\bar{2}2)$ and $(\bar{1}\bar{1}22)$ faces, which are the growth interfaces in the $+S$- and $-S$-regions in Al-doped Y-bar synthetic quartz. We must emphasize that the S-cut seed grows on the $(11\bar{2}1)$ and $(\bar{1}\bar{1}21)$ faces, but there is no corresponding growth region in the Y-bar synthetic quartz because the growth interfaces of $+S$- and $-S$-regions are unrelated to these faces, as described in the previous section. The growth direction perpendicular to the X-cut and Z-cut correspond to the $+X$-, $-X$-, and two Z-regions, respectively.

It is known that H impurity in quartz produces OH bonds which are detected by infrared absorption. The infrared absorption characteristic shows a broad band at the 3400 l/cm wave number region supperposed upon several sharp bands. In Fig. 4, a typical infrared spectrum is shown. At room temperature, broad band B and only one sharp band S are observed, even though many sharp bands are detected at low temperatures. P, Q and R were assigned to the overtone and/or combination bands of the Si-O vibrations.[8] Here, we noted broad band B because it has remarkable anisotropy in relation to the growth direction and is easily observed at room temperature. Quantitative analysis is possible by applying Paterson's formula given by eq. (1), which was proposed for the broad band absorption analysis:[9]

$$C=(1/50)\int\{K(w)/(3780-w)\}\,dw, \tag{1}$$

where C is the H impurity content in mol H/l, K is the absorption coefficient in l/cm and w is the wave number in l/cm. In order to evaluate the value of C, the numerical integration was adopted in the present study, as shown in eq. (2):

$$C=(1/50)\sum\{K(w)/(3780-w)\}\Delta w, \tag{2}$$

Here, the values of $K(w)$ for each corresponding value of w can be read out from infrared absorption spectra in

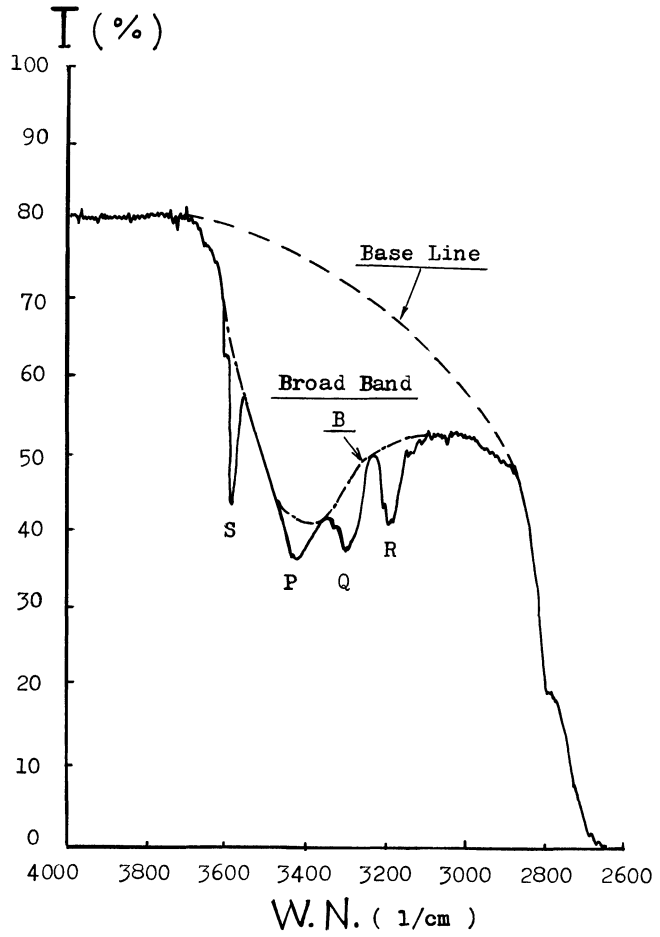

Fig. 4. Percent transmission (T) and wave number (W.N.) characteristics observed in the sample of $-\xi(\bar{1}\bar{1}22)$ growth.

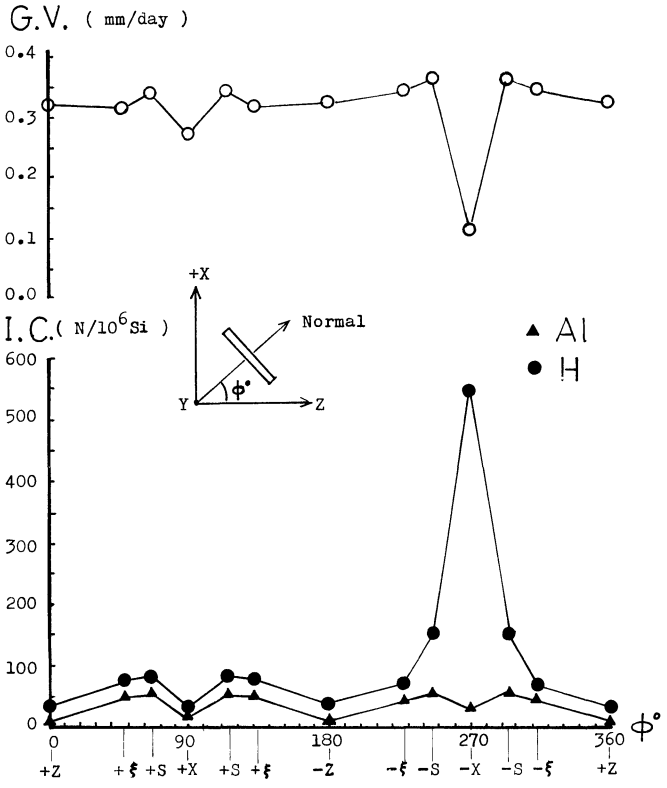

Fig. 5. Relationship between impurity content (I.C.) and growth velocity (G.V.).

each interval of Δw. In the present case, infrared spectra show $T\%$ (percent transmission) as a function of W. In order to estimate $K(w)$, we must estimate the base and the absorption lines corresponding to the broad band without criterions. Here, the "French curve"[10] was used in most cases. The interval, Δw, was chosen as 40 l/cm, because it had sufficient accuracy under the present analytical technique.

Figure 5 shows the relationship between Al and H (for the broad band) impurity contents and the growth velocity as a function of the growth direction. The growth direction is presented as ϕ, which corresponds to the angle between the Z-axis and the seed normal. Both Al and H impurities were evaluated as the number of atoms per 10^6 Si atoms. The growth velocity is defined to be the distance between the seed surface and the crystal surface divided by the growth period and evaluated to be mm/day. An approximate correlation was observed between growth velocity and impurity contents, except for the H impurity content in the $-X$-growth direction. In the $-X$-direction, Al content is lower than the $-S$- and $-\xi$-directions, but H content shows an extremely high value. It is also observed that the growth velocity of the $-X$-direction is the slowest. The growth interface is supposed to be covered by H_2O, which acts as an impurity and suppresses the growth rate. It was reported that dehydration on the growth interface limits the growth process in a hydrothermal condition.[11] The impurity segregation characteristic obtained in the present study suggests that the $-X$-face, $(\bar{1}\bar{1}20)$, attracts more H_2O molecules than $+X$-faces, $(11\bar{2}0)$. In quartz, the two faces sperpendicular to a polar axis such as the X-axis are not equivalent and have a different atomic arrangement. Therefore, it is natural to consider that the two faces have a different amount of adsorbed H_2O molecules. The same phenomenon is also observed between the $+S$-face, $(11\bar{2}1)$, and the $-S$-face, $(\bar{1}\bar{1}2\bar{1})$; i.e., the $-S$-growth region contains more H impurity than the $+S$-growth region. In the case of the ξ-cut, there is no significant difference between the $+\xi$-face, $(11\bar{2}2)$, and the $-\xi$-face, $(\bar{1}\bar{1}2\bar{2})$. Therefore, it is emphasized that the difference of H content between + and -faces decreases with departure from the polar axis. The $-S$-growth region contains a smaller amount of H impurity than the $-X$-growth region and does not have any influence on the growth velocity.

Al with 3+ valence is thought to easily substitute for Si with 4+ valence in quartz, and thus this needs an additional positive charge for the charge balance. H, Li and Na at interstitial sites and the hole trapped at the oxygen play the role of compensators.[12] The studies of electron spin resonance and infrared absorption at low temperatures showed that the Al–M state (M=Li and Na) is common but Al–H does not exist in as-grown synthetic quartz grown in alkali solution. Al–H is observed only after γ-irradiation. Al(e+) which corresponds to the hole trapped at oxygen is also produced by γ-irradiation. Therefore, the impurity state of H analyzed by infrared absorption spectroscopy in the present work is considered to be independent of the Al impurity analyzed by atomic absorption spectroscopy. Especially in the $-X$-region, the amount of H impurity is much larger than that of the Al impurity. Moreover, recent results of near-infrared spectroscopy showed that the broad band corresponds mainly to H_2O rather than OH.[13]

Therefore, the adsorbed H_2O molecules on the growth interface are supposed to enter the structural channels in the crystal lattice as interstitial H_2O impurity.

§4. Summary

The present results are summarized as follows: The $-X$-direction has the lowest growth velocity among the perpendicular directions of the Y-axis, due to the effect of H_2O adsorbed on the growth interface under the hydrothermal condition. Therefore, the $-X$-face, $(\bar{1}\bar{1}20)$, always becomes larger in size. The Al impurity has the effect, on $(11\bar{2}2)$ and $(\bar{1}\bar{1}2\bar{2})$, of suppressing the growth velocities. However, this effect is controllable by the Al content in the nutrient. It should be noted that the so-called S-region in Y-bar synthetic quartz is independent of the $(11\bar{2}1)$ face, which is designated as the S-face in natural quartz.

Acknowledgments

The authors are indebted to M. Kurashige for the preparation of Al-doped synthetic quartz. Growth experiments were performed in collaboration with ABC XTAL Microeletronica S.A.

References

1) F. Iwasaki, H. Iwasaki and C. K. Suzuki: Jpn. J. Appl. Phys. **28** (1989) 68.
2) F. Iwasaki and K. Kurashige: Jpn. J. Appl. Phys. **17** (1978) 817.
3) D. Chakraborty and G. Lehmann: J. Solid State Chem. **17** (1976) 305.
4) H. Iwasaki, F. Iwasaki, C. K. Suzuki, V. A. R. Oliverira, D. C. A. Hummel and A. H. Shinohara: *Proc. 40th Ann. Symp. Freq. Control, Philadelphia, 1986* (IEEE, NJ, 1986) p. 39.
5) C. K. Suzuki, A. H. Shinohara, V. A. R. Oliveira, S. M. Takia and J. Kiss: *Proc. 40th Ann. Symp. Freq. Control, Philadelphia, 1986* (IEEE, NJ, 1986) p. 47.
6) C. Frondel: *The System of Mineralogy Vol. 3, Silica Mineral* (John Wiley & Sons, New York, 1962) 7th ed., p. 36.
7) S. Taki and M. Hosaka: Hydrothermal **1** (1983) 15. [in Japanese].
8) S. Kats: Philips Res. Repts. **17** (1962) 133.
9) M. S. Paterson: Bull. Mineral. **105** (1982) 20.
10) S. Newman, E. M. Stolper and S. Epstein: Am. Mineral. **71** (1985) 1527.
11) A. A. Chernov and V. A. Kuznetsov: Sov. Phys.-Crystallogr. **14** (1970) 753.
12) L. E. Halliburton, N. Koumvakalis, M. E. Markes and J. J. Martin: J. Appl. Phys. **52** (1981) 3565.
13) R. D. Aines, S. H. Kirby and G. R. Sossman: Phys. Chem. Minerall **11** (1984) 204.